Copyright © 2012 Tech Science Press CMC, vol.29, no.3, pp.279-298, 2012

Local Electroelastic Field and Effective Electroelastic Moduli of Piezoelectric Nanocomposites with Interface Effect

Shasha Yang[1], **Shuling Hu**[1] **and Shengping Shen**[1,2]

Abstract: Due to the large ratio of surface area to volume in nanoscale objects, the property of surfaces and interfaces likely becomes a prominent factor in controlling the behavior of nano-heterogeneous materials. In this work, based on the Gurtin-Murdoch surface/interface elastic theory, a distinct expression is derived for embedded nano-inclusion in an infinite piezoelectric matrix coupled with interface effect. For the problem of a spherical inclusion in transversely isotropic piezoelectric medium, we reach a conclusion that the elastic and electric field are uniform when eigen-strain and eigen-electric field imposed on the inclusion are uniform even in the presence of the interface influence. The electroelastic fields in the inclusion are related to both interface electroelastic parameters and the radius of the inclusion. Then overall properties of the composites are estimated by using the dilute distribution model. Numerical results reveal that the effective electroelastic moduli are function of the interface parameters and the size of the nano-inhomogeneities.

Keywords: Nanocomposites; Piezoelectrics; Green's function; Interface effect

1 Introduction

Along with advances in nanotechnology, many investigations are devoted to nanoscale science and developments of nanocomposites. Nanocomposites are of interest because of their unusual mechanical, thermal, electrical, optical and magnetic properties (Cherkaoui and Capolungo, 2009; Hu and Shen, 2010; Shen and Hu, 2010; Xu and Shen, 2012). That is because, when the size is on nanoscale, the property of surfaces and interfaces becomes a prominent factor in controlling the whole behavior due to the large ratio of surface/interface to volume.

[1] State Key Laboratory for Strength and Vibration of Mechanical Structures, School of Aerospace, Xi'an Jiaotong University, Xi'an 710049, China

[2] Corresponding author. Tel./fax: +862982660977. *E-mail address*: sshen@mail.xjtu.edu.cn (S. Shen).

Many studies focused on the effect of surface/interface on the elastic properties of nanocomposites. The work of Sharma et al. (2003) is one of the pioneering works to combine surface elasticity with Eshelby's formalism to nanoinhomogeneity problem. They derived the closed-form expression for the elastic state of spherical inhomogeneities with surface effects using a variational formulation. Then Sharma and Ganti (2004) modified the classical formulation of Eshelby for embedded inclusions by incorporating the interface effect. They proved that only inclusions of a constant curvature admit a uniform elastic state under uniform eigenstrains coupled with interface elasticity. Duan et al. (2005b) extended the Eshelby formalism to nano-inhomogeneities. Duan et al. (2005a) also investigated the general micromechanical framework for the prediction of the effective elastic moduli of the heterogeneous materials containing spherical nanoinhomogeneities. In 2008, Duan et al. (2008) gave a review article about how to extend the classical theory of elasticity to nanoscale. Lim et al. (2006) analyzed the influence of interface stress on the elastic field within a nanoscale inclusion when the eigenstrain is non-hydrostatic. Yang (2006) gave the effective bulk modulus of a composite consisting of spherical inclusions at dilute concentrations, in which the surface effect is simply simulated by a constant residual tension. Huang et al. (Huang and Sun, 2007; Huang and Wang, 2007) considered the change of the elastic fields induced by the interface energy and interface stresses using the finite deformation theory. They thought during the deformation process, the size, the shape and the curvature tensor of the interface will change, which is different from Sharma and Ganti (2004) and Duan et al. (2005a). Tian and Rajapakse (2007) studied the two-dimensional elastic field of a nanoscale elliptical inhomogeneity embedded in an infinite matrix under arbitrary remote loading and a uniform eigenstrain by complex potential function method. Chen et al. (Chen et al., 2007; Chen and Dvorak, 2006; Chen et al., 2007) predicted the effective elastic moduli of the heterogeneous materials containing nano-inhomogeneities. All the studies indicate that the surface/interface effect is important to the mechanical behavior of nanocomposites.

In addition to the elastic behavior, lots of theoretical and technological interests focused on piezoelectric nanomaterials and nanocomposites recently. For examples, Huang and Yu (2006) gave the stress and electric fields in a piezoelectric ring under prescribed electric potential based on the surface piezoelectricity. Chen (2008) considered the macroscopic behavior of two-phase fibrous piezoelectric composites. Xiao et al. (2011) studied the nanocomposites under far-field antiplane mechanical load and inplane electric load. The present work concerns with the fundamental solution of the electroelastic fields incorporating the interface effect by means of Green's function methods. Additionally, the influence of the interface electroelastic modulus on the overall effective modulus is discussed in detail, which has not been

analyzed yet in previous articles.

The paper is organized as follows. In Sec.2, we derive the general formulas of the electroelastic fields for nanoinclusion embedded in an infinite piezoelectric matrix including the interface effect. We obtain the closed form of the electroelastic fields within the spherical inclusion under some assumption in Sec.3. Based on the equivalent inclusion method, effective electroelastic constants are investigated by using dilute schemes in Sec.4. In Sec.5, the size effects on local electroelastic fields and effective electroelastic moduli are numerically discussed and illustrated. Finally, concluding remarks are made in Sec.6.

2 General formulas

The composite under consideration consists of a piezoelectric matrix in which an arbitrary shaped inclusion are embedded. We suppose a prescribed uniform eigen-strain $\boldsymbol{\varepsilon}^*$ and uniform eigen-electric field $\mathbf{E}^*$ within the domain of the inclusion. The constitutive relations in the bulk piezoelectric materials are written as:

$$\boldsymbol{\sigma}^B = \mathbf{c} : \boldsymbol{\varepsilon} - \mathbf{e} \cdot \mathbf{E} \tag{1}$$

$$\mathbf{D}^B = \mathbf{e} : \boldsymbol{\varepsilon} + \boldsymbol{\kappa} \cdot \mathbf{E} \tag{2}$$

where $\mathbf{c}$, $\mathbf{e}$ and $\boldsymbol{\kappa}$ being the bulk elastic, piezoelectric and dielectric tensors. The superscript "B" represents the quantity on the bulk.

If the free charges and body forces do not exist, the equilibrium and Gauss equations can be written as :

$$\nabla \cdot \boldsymbol{\sigma}^B = 0 \tag{3}$$

$$\nabla \cdot \mathbf{D}^B = 0 \tag{4}$$

As a departure from the classical solution, the interface Π between the inclusion and matrix is endowed with a deformation-dependent interfacial energy Γ. Here, we first introduce the tangent projection operator $\mathbf{p}^s$ of the interface Π. It is defined by Gurtin et al. (1998):

$$\mathbf{p}^s = \mathbf{I} - \mathbf{n} \otimes \mathbf{n} \tag{5}$$

Here, $\mathbf{I}$ is the three-dimensional identity tensor and $\mathbf{n}$ is the unit normal vector on the interface. This surface projection tensor maps tensor fields from bulk to surface. In Gurtin et al. (1998), the interface is assumed to be coherent in which no atomic bonds are broken. The coherency implies that the tangential projection of strain and the tangential components of electric field are continuous across Π. So, the

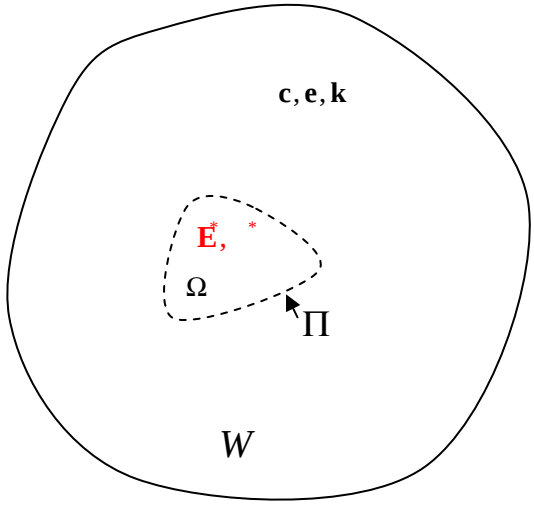

Figure 1: Schematic of the problem

interface can be considered as a material surface and every point $\mathbf{x}$ of Π is endowed with a surface strain $\boldsymbol{\varepsilon}^s = \mathbf{p}^s \boldsymbol{\varepsilon} \mathbf{p}^s$, a surface stress $\boldsymbol{\sigma}^s$, a surface electric field $\mathbf{E}^s = \mathbf{p}^s \mathbf{E}$ and a surface electric displacement $\mathbf{D}^s$. As proposed by Huang and Yu (2006), the constitutive equations for the surface are expressed as:

$$\boldsymbol{\sigma}^s = \boldsymbol{\sigma}^0 + \mathbf{c}^s : \boldsymbol{\varepsilon}^s - \mathbf{e}^s \cdot \mathbf{E}^s \tag{6}$$

$$\mathbf{D}^s = \mathbf{D}^0 + \mathbf{e}^s : \boldsymbol{\varepsilon}^s + \boldsymbol{\kappa}^s \cdot \mathbf{E}^s \tag{7}$$

where $\boldsymbol{\sigma}^0$ and $\mathbf{D}^0$ can be termed as residual surface stress and residual surface electric displacement without applied strain and electric field, and $\mathbf{c}^s$, $\mathbf{e}^s$ and $\boldsymbol{\kappa}^s$ are surface elastic moduli, surface piezoelectric tensor and surface dielectric tensor. The superscript "s" represents the quantity on the surface.

Hu and Shen (2009) gave the generalized electromechanical Young-Laplace equations with surface and gradient effects, as well as effect of electrostatic force. In this paper, we use the results only considering the surface/interface effect, which can be written as

$$\left(\boldsymbol{\sigma}^M - \boldsymbol{\sigma}^I\right) \cdot \mathbf{n} = -\mathrm{div}_s \boldsymbol{\sigma}^s \tag{8}$$

$$\left(\mathbf{D}^M - \mathbf{D}^I\right) \cdot \mathbf{n} = -\mathrm{div}_s \mathbf{D}^s \tag{9}$$

Here the superscript "M" and "I" mean the matrix and the inclusion respectively, which both are the bulk quantities. Eq. (8) and Eq. (9) connect the bulk quantities and the interface quantities which are significant in the following derivation.

Notes that the eigen-value is only nonzero within the inclusion domain, introducing the characteristic function $H(\mathbf{x})$ of Ω (see in Fig.1) as:

$$\begin{cases} H(\mathbf{x}) = 1 | \mathbf{x} \in \Omega \\ H(\mathbf{x}) = 0 | \mathbf{x} \notin \Omega \end{cases} \tag{10}$$

so the whole constitutive law for the inclusion-matrix is given by

$$\begin{cases} \boldsymbol{\sigma}^B = \mathbf{c} : \{\boldsymbol{\varepsilon} - \boldsymbol{\varepsilon}^* H(\mathbf{x})\} - \mathbf{e} \cdot \{\mathbf{E} - \mathbf{E}^* H(\mathbf{x})\} \\ \mathbf{D}^B = \mathbf{e} : \{\boldsymbol{\varepsilon} - \boldsymbol{\varepsilon}^* H(\mathbf{x})\} + \boldsymbol{\kappa} \cdot \{\mathbf{E} - \mathbf{E}^* H(\mathbf{x})\} \end{cases} \tag{11}$$

Analogous to Sharma and Ganti (2004), substituting Eq. (11) into Eq. (3) and Eq. (4), and accounting for the discontinuity of $\sigma(\mathbf{x})$ and $\mathbf{D}(\mathbf{x})$ across the interface Π yield:

$$\begin{aligned} &\nabla \cdot \boldsymbol{\sigma}^B = \\ &\nabla \cdot (\mathbf{c} : \boldsymbol{\varepsilon}) - \nabla \cdot \{\mathbf{c} : \boldsymbol{\varepsilon}^* H(\mathbf{x})\} - \nabla \cdot (\mathbf{e} \cdot \mathbf{E}) + \nabla \cdot \{\mathbf{e} \cdot \mathbf{E}^* H(\mathbf{x})\} - (\sigma^M - \boldsymbol{\sigma}^I) \cdot \mathbf{n} \delta_\Pi(\mathbf{x}) \\ &= 0 \end{aligned} \tag{12}$$

$$\begin{aligned} &\nabla \cdot \mathbf{D}^B = \\ &\nabla \cdot (\mathbf{e} : \boldsymbol{\varepsilon}) - \nabla \cdot \{\mathbf{e} : \boldsymbol{\varepsilon}^* H(\mathbf{x})\} + \nabla \cdot (\boldsymbol{\kappa} \cdot \mathbf{E}) - \nabla \cdot \{\boldsymbol{\kappa} \cdot \mathbf{E}^* H(\mathbf{x})\} - (\mathbf{D}^M - \mathbf{D}^I) \cdot \mathbf{n} \delta_\Pi(\mathbf{x}) \\ &= 0 \end{aligned} \tag{13}$$

where $\delta_\Pi(\mathbf{x})$ is the Dirac delta function defined on Π.

Coupling the generalized electromechanical Young-Laplace equations , Eq. (12) and Eq. (13) can be rewritten as:

$$\nabla \cdot (\mathbf{c} : \boldsymbol{\varepsilon}) - \nabla \cdot (\mathbf{e} \cdot \mathbf{E}) = \underbrace{\nabla \cdot \{\mathbf{c} : \boldsymbol{\varepsilon}^* H(\mathbf{x})\} - \nabla \cdot \{\mathbf{e} \cdot \mathbf{E}^* H(\mathbf{x})\}} - \underbrace{\mathrm{div}_s \boldsymbol{\sigma}^s \delta_\Pi(\mathbf{x})} \tag{14}$$

$$\nabla \cdot (\mathbf{e} : \boldsymbol{\varepsilon}) + \nabla \cdot (\boldsymbol{\kappa} \cdot \mathbf{E}) = \underbrace{\nabla \cdot \{\mathbf{e} : \boldsymbol{\varepsilon}^* H(\mathbf{x})\} + \nabla \cdot \{\boldsymbol{\kappa} \cdot \mathbf{E}^* H(\mathbf{x})\}} - \underbrace{\mathrm{div}_s \mathbf{D}^s \delta_\Pi(\mathbf{x})} \tag{15}$$

Obviously, the right hand side of the equations contain the eigen items caused by $\boldsymbol{\varepsilon}^*$ and $\mathbf{E}^*$, and the interface items caused by $\boldsymbol{\sigma}^s$ and $\mathbf{D}^s$. Analogous to Sharma and Ganti (2004), treating the underlined terms as body force and body electric charge respectively, in conjunction with the piezoelectric Green's function, we can write the displacement field and electric potential due to the eigenfield and interface

effect as

$$\begin{aligned}\mathbf{u}(\mathbf{x}) &= -\int_V \mathbf{G}^1(\mathbf{y}-\mathbf{x})(\nabla\cdot\{\mathbf{c}:\boldsymbol{\varepsilon}^* H(\mathbf{y})\} - \nabla\cdot\{\mathbf{e}\cdot\mathbf{E}^* H(\mathbf{y})\})dV(\mathbf{y}) \\ &-\int_V \mathbf{G}^2(\mathbf{y}-\mathbf{x})(\nabla\cdot\{\mathbf{e}:\boldsymbol{\varepsilon}^* H(\mathbf{y})\} + \nabla\cdot\{\boldsymbol{\kappa}\cdot\mathbf{E}^* H(\mathbf{y})\})dV(\mathbf{y}) \\ &+\int_\Pi \mathbf{G}^1(\mathbf{y}-\mathbf{x})\mathrm{div_s}\boldsymbol{\sigma}^s(\mathbf{y})dS(\mathbf{y}) + \int_\Pi \mathbf{G}^2(\mathbf{y}-\mathbf{x})\mathbf{div_s}\mathbf{D}^s(\mathbf{y})dS(\mathbf{y})\end{aligned} \tag{16}$$

$$\begin{aligned}\Phi(\mathbf{x}) &= -\int_V \mathbf{G}^3(\mathbf{y}-\mathbf{x})(\nabla\cdot\{\mathbf{c}:\boldsymbol{\varepsilon}^* H(\mathbf{y})\} - \nabla\cdot\{\mathbf{e}\cdot\mathbf{E}^* H(\mathbf{y})\})dV(\mathbf{y}) \\ &-\int_V \mathbf{G}^4(\mathbf{y}-\mathbf{x})(\nabla\cdot\{\mathbf{e}:\boldsymbol{\varepsilon}^* H(\mathbf{y})\} + \nabla\cdot\{\boldsymbol{\kappa}\cdot\mathbf{E}^* H(\mathbf{y})\})dV(\mathbf{y}) \\ &+\int_\Pi \mathbf{G}^3(\mathbf{y}-\mathbf{x})\mathrm{div_s}\boldsymbol{\sigma}^s(\mathbf{y})dS(\mathbf{y}) + \int_\Pi \mathbf{G}^4(\mathbf{y}-\mathbf{x})\mathrm{div_s}\mathbf{D}^s(\mathbf{y})dS(\mathbf{y})\end{aligned} \tag{17}$$

Here $\mathbf{G}^1, \mathbf{G}^2, \mathbf{G}^3, \mathbf{G}^4$ are Green's tensors for classical piezoelectrics (see in Appendix). We make use of Gauss theorem to cast Eq. (16) and Eq. (17) in more explicit forms:

$$\begin{aligned}\mathbf{u} &= -\int_\Omega (\nabla_x \otimes \mathbf{G}^1):(\mathbf{c}:\boldsymbol{\varepsilon}^* - \mathbf{e}\cdot\mathbf{E}^*)dV - \int_\Omega (\nabla_x \otimes \mathbf{G}^2)\cdot[\mathbf{e}:\boldsymbol{\varepsilon}^* + \mathbf{k}\cdot\mathbf{E}^*]dV \\ &+\int_\Pi \mathbf{G}^1\cdot\mathrm{div_s}\sigma^s dS + \int_\Pi \mathbf{G}^2\mathrm{div_s}\mathbf{D}^s dS\end{aligned} \tag{18}$$

$$\begin{aligned}\Phi &= -\int_\Omega (\nabla_x \otimes \mathbf{G}^3):(\mathbf{c}:\boldsymbol{\varepsilon}^* - \mathbf{e}\cdot\mathbf{E}^*)dV - \int_\Omega (\nabla_x \otimes \mathbf{G}^4)\cdot[\mathbf{e}:\boldsymbol{\varepsilon}^* + \mathbf{k}\cdot\mathbf{E}^*]dV \\ &+\int_\Pi \mathbf{G}^3\cdot\mathrm{div_s}\sigma^s dS + \int_\Pi \mathbf{G}^4\mathrm{div_s}\mathbf{D}^s dS\end{aligned} \tag{19}$$

In the derivation of Eq. (18) and Eq. (19), the relation $\frac{\partial \mathbf{G}^i(\mathbf{y}-\mathbf{x})}{\partial \mathbf{y}} = -\frac{\partial \mathbf{G}^i(\mathbf{y}-\mathbf{x})}{\partial \mathbf{x}}$ (i=1, 2, 3, 4) and the fact that Green's functions are equal to zero at infinity are also used. Correspondingly, the resulting strain field and electric field components are given by:

$$\begin{aligned}\boldsymbol{\varepsilon}(\mathbf{x}) &= \mathbf{S}^1:\boldsymbol{\varepsilon}^* - \mathbf{S}^2\cdot\mathbf{E}^* \\ &+\mathrm{sym}\left\{\nabla_x \otimes \int_\Pi \mathbf{G}^1\cdot\mathrm{div_s}\boldsymbol{\sigma}^s dS\right\} + \mathrm{sym}\left\{\nabla_x \otimes \int_\Pi \mathbf{G}^2\mathrm{div_s}\mathbf{D}^s dS\right\}\end{aligned} \tag{20}$$

$$\begin{aligned}\mathbf{E}(\mathbf{x}) &= -\mathbf{S}^3:\boldsymbol{\varepsilon}^* + \mathbf{S}^4\cdot\mathbf{E}^* \\ &-\left\{\nabla_x \otimes \int_\Pi \mathbf{G}^3\cdot\mathrm{div_s}\boldsymbol{\sigma}^s dS\right\} - \left\{\nabla_x \otimes \int_\Pi \mathbf{G}^4\mathrm{div_s}\mathbf{D}^s dS\right\}\end{aligned} \tag{21}$$

Here $\mathbf{S}^1, \mathbf{S}^2, \mathbf{S}^3, \mathbf{S}^4$ are piezoelectric Eshelby tensors (see in Appendix). The relation between piezoelectric Green's function and Eshelby tensors are also revealed in Appendix. The notation sym $\{\cdot\}$ represents the symmetric part of the quantities.

Until now, we obtained the general expressions of strain and electric fields in the piezoelectric composites incorporating interface effects. The equations are implicit since the interface stress and interface electric displacement are related to bulk strain and bulk electric field. Without additional assumption, further simplification seems to be infeasible. So particular case are studied in detail in the next section.

3 Local electroelastic fields

When dealing with piezoelectric solids, transverse isotropy is of fundamental important in technology. So we assume the material is transversely isotropic. Here, the shape of the inclusion is spherical which are endowed with a constant curvature. Here again, $\boldsymbol{\varepsilon}^*$ and $\mathbf{E}^*$ will be uniformly distributed in subdomain Ω and vanish outside Ω. Since the medium is transverse isotropic, the interface can be regarded as isotropic. That means, the surface piezoelectric constant can be neglected. Meanwhile, if the deformation is infinitesimal, the contribution of $\boldsymbol{\varepsilon}^s$ is negligibly small compared to the residue surface stress .(Yang, 2006). To simplify the derivation, we set $\mathbf{D}^0 = 0$ in this paper. Thus, the constitutive equation for the interface can be reduced to:

$$\boldsymbol{\sigma}^s = \boldsymbol{\sigma}^0 \tag{22}$$

$$\mathbf{D}^s = \boldsymbol{\kappa}^s \cdot \mathbf{E}^s \tag{23}$$

Now a series of calculations will be exhibited to derive the strain and electric field within a spherical inclusion. First, we calculate the right items of Eq. (20) and Eq. (21) for a constant electric field $\mathbf{E}(\mathbf{x}) = \mathbf{E}^\Omega$ inside the inclusion.

According to Sharma and Ganti (2004) and Quang et al. (2010), the surface divergence of $\boldsymbol{\sigma}^s$ and $\mathbf{D}^s$ are obtained as:

$$div_s\boldsymbol{\sigma}^s = div_s(\sigma^0\mathbf{p}^s) = \sigma^0 div_s\mathbf{p}^s = 2\sigma^0\lambda\mathbf{n} \tag{24}$$

$$div_s\mathbf{D}^s = -2\lambda k^s\mathbf{E}^\Omega \cdot \mathbf{n} \tag{25}$$

where λ is the mean curvature of the inclusion. Here $\lambda = 1/R_0$ for spheres where R_0 is the radius. In addition, $\boldsymbol{\kappa}^s = k^s\mathbf{P}^s$ for the point $\mathbf{x}$ on the interface Π.

Substituting Eq. (24) and Eq. (25) into Eq. (20) and Eq. (21), and using the divergence theorem, the third term on the right hand side of Eq. (20) can be obtained as

following:

$$\begin{aligned}
&\mathrm{sym}\left\{\nabla_x \otimes \int_{\Pi} \mathbf{G}^1 \cdot \mathrm{div_s}\boldsymbol{\sigma}^s dS\right\} = \mathrm{sym}\left\{\nabla_x \otimes \int_{\Pi} G_{mj}(y-x) 2\sigma^0 \lambda n_j dS(y)\right\} \\
&= (2\sigma^0\lambda)\mathrm{sym}\left\{\nabla_x \otimes \int_{\Pi} G_{mj}(y-x) n_j dS(y)\right\} \\
&= (2\sigma^0\lambda)\mathrm{sym}\left\{\nabla_x \otimes \int_{\Omega} \nabla \cdot \mathbf{G}^1(\mathbf{y}-\mathbf{x}) dV(\mathbf{y})\right\} \\
&= -\mathrm{sym}\left\{\nabla_x \otimes \int_{\Omega} \nabla_x \otimes \mathbf{G}^1(\mathbf{y}-\mathbf{x}) dV(\mathbf{y})\right\} : (2\sigma^0\lambda)\mathbf{I} = (2\sigma^0\lambda)\mathbf{T}^1 : \mathbf{I}
\end{aligned} \tag{26}$$

The fourth term on the right hand side of Eq. (20) is :

$$\begin{aligned}
&\mathrm{sym}\left\{\nabla_x \otimes \int_{\Pi} \mathbf{G}^2 \mathrm{div_s}\mathbf{D}^s dS\right\} = -(2\lambda k^s)\mathrm{sym}\left\{\nabla_x \otimes \int_{\Pi} G_{m4}(y-x) E_i^{\Omega} n_i dS(y)\right\} \\
&= -(2\lambda k^s)\mathrm{sym}\left\{\nabla_x \otimes \int_{\Omega} (G_{m4}(y-x) E_i^{\Omega})_{,i} dV(y)\right\} \\
&= -(2\lambda k^s)\mathrm{sym}\left\{\nabla_x \otimes \int_{\Omega} [G_{m4,i}(y-x) E_i^{\Omega} + G_{m4}(y-x) E_{i,i}^{\Omega}] dV(y)\right\} \\
&= (2\lambda k^s)\mathrm{sym}\left\{\nabla_x \otimes \int_{\Omega} \nabla_x \otimes \mathbf{G}^2(\mathbf{y}-\mathbf{x}) dV(\mathbf{y})\right\} \cdot \mathbf{E}^{\Omega} = (-2\lambda k^s)\mathbf{T}^2 \cdot \mathbf{E}^{\Omega}
\end{aligned} \tag{27}$$

Similarly, the third term on the right hand side of Eq. (21) can be written as:

$$\begin{aligned}
&-\left\{\nabla_x \otimes \int_{\Pi} \mathbf{G}^3 \cdot \mathrm{div_s}\boldsymbol{\sigma}^s dS\right\} \\
&= -(2\sigma^0\lambda)\left\{\nabla_x \otimes \int_{\Pi} G_{4j}(y-x) n_j dS(y)\right\} = (-2\sigma^0\lambda)\mathbf{T}^3 : \mathbf{I}
\end{aligned} \tag{28}$$

The fourth term on the right hand side of Eq. (21) is:

$$\begin{aligned}
&-\left\{\nabla_x \otimes \int_{\Pi} \mathbf{G}^4 \mathrm{div_s}\mathbf{D}^s dS\right\} \\
&= (2\lambda k^s)\left\{\nabla_x \otimes \int_{\Pi} G_{44}(y-x) E_i^{\Omega} n_i dS(y)\right\} = (2\lambda k^s)\mathbf{T}^4 \cdot \mathbf{E}^{\Omega}
\end{aligned} \tag{29}$$

Here, the four interaction tensors $\mathbf{T}^1$, $\mathbf{T}^2$, $\mathbf{T}^3$, $\mathbf{T}^4$ are related to piezoelectric Eshelby tensors $\mathbf{S}^1$, $\mathbf{S}^2$, $\mathbf{S}^3$, $\mathbf{S}^4$. The explicit expressions of these tensors are elaborated in Appendix. Then Eq. (20) and Eq. (21) can be reduced to

$$\boldsymbol{\varepsilon}(\mathbf{x}) = \mathbf{S}^1 : \boldsymbol{\varepsilon}^* - \mathbf{S}^2 \cdot \mathbf{E}^* + (\frac{2\sigma^0}{R_0})\mathbf{T}^1 : \mathbf{I} - (\frac{2k^s}{R_0})\mathbf{T}^2 \cdot \mathbf{E}^{\Omega} \tag{30}$$

$$\mathbf{E}(\mathbf{x}) = -\mathbf{S}^3 : \boldsymbol{\varepsilon}^* + \mathbf{S}^4 \cdot \mathbf{E}^* - (\frac{2\sigma^0}{R_0})\mathbf{T}^3 : \mathbf{I} + (\frac{2k^s}{R_0})\mathrm{T}^4 \cdot \mathbf{E}^\Omega \tag{31}$$

If the electric field is constant within the inclusion, $\mathbf{E}(\mathbf{x})$ must be identical to $\mathbf{E}^\Omega$ for $\mathbf{x}$ inside the inclusion. Thus, we have:

$$\mathbf{E}(\mathbf{x})|_{x\in\Omega} = -\mathbf{S}^3 : \boldsymbol{\varepsilon}^* + \mathbf{S}^4 \cdot \mathbf{E}^* - (\frac{2\sigma^0}{R_0})\mathbf{T}^3 : \mathbf{I} + (\frac{2k^s}{R_0})\mathbf{T}^4 \cdot \mathbf{E}^\Omega = \mathbf{E}^\Omega \tag{32}$$

For $\mathbf{x}$ within the spherical inclusion, the classical piezoelectric Eshelby tensors $\mathbf{S}^1, \mathbf{S}^2, \mathbf{S}^3, \mathbf{S}^4$ are all constant tensors in the classical piezoelectric theory (Wang, 1992; Dunn and Taya, 1993; Dunn and Wienecke, 1997). So, form Eq. (32) we can get the conclusion that in this particular case, the electric fields within the inclusion are uniform even including interface effect. When $\mathbf{E}^\Omega$ =constant, it is easy to get that:

$$\boldsymbol{\varepsilon}(\mathbf{x})|_{x\in\Omega} \equiv \boldsymbol{\varepsilon}^\Omega = \mathbf{S}^1 : \boldsymbol{\varepsilon}^* - \mathbf{S}^2 \cdot \mathbf{E}^* + (\frac{2\sigma^0}{R_0})\mathbf{T}^1 : \mathbf{I} - (\frac{2k^s}{R_0})\mathbf{T}^2 \cdot \mathbf{E}^\Omega = \text{constant} \tag{33}$$

This is the strain field within the inclusion, and is also identically uniform when concerning interface effect. Moreover, we emphasize that the conclusion that electroelastic fields are uniform inside the inclusion is only established under the assumptions in this section.

4 Effective electroelastic moduli

Since for a spherical inclusion, strain and electric fields with interface effect are uniform, the equivalent inclusion method can be easily applied to investigate piezoelectric inhomogeneities. At the macroscopic scale, the composite is assumed to be statistically homogeneous. The corresponding effective moduli are characterized by:

$$\tilde{\boldsymbol{\sigma}} = \overline{\mathbf{c}^*}\langle\boldsymbol{\varepsilon}\rangle - \overline{\mathbf{e}^*}\langle\mathbf{E}\rangle \tag{34}$$

$$\tilde{\mathbf{D}} = \overline{\mathbf{e}^*}\langle\boldsymbol{\varepsilon}\rangle + \overline{\mathbf{k}^*}\langle\mathbf{E}\rangle \tag{35}$$

where $\overline{c^*}, \overline{e^*}, \overline{k^*}$ are effective elastic, piezoelectric and dielectric constants with interface effect, respectively. $\tilde{\sigma}, \tilde{\mathbf{D}}$ denote the macroscopic stress and electric displacement respectively. Here, the symbol <> denotes the volume average. According to Duan et al. (2005a) and Quang et al. (2010), unlike the classical case where the matrix-inclusion interface is perfect, the macroscopic stress and electric displacement can be determined by:

$$\tilde{\boldsymbol{\sigma}} = \langle\boldsymbol{\sigma}\rangle + \frac{1}{V}\int_{\Pi} (\boldsymbol{\sigma}^M - \boldsymbol{\sigma}^I) \cdot \mathbf{n}\mathbf{x} d\mathbf{x} \tag{36}$$

$$\tilde{\mathbf{D}} = \langle \mathbf{D} \rangle + \frac{1}{V} \int_{\Pi} (\mathbf{D}^M - \mathbf{D}^I) \cdot \mathbf{n}\mathbf{x} d\mathbf{x} \tag{37}$$

Here, V denotes the volume of the domain W, and W is the representative volume element (see in Figure 2). Compared with the classical case, a new term due to the discontinuity of $\sigma(\mathbf{x})$ and $\mathbf{D}(\mathbf{x})$ across the interface Π appears in Eq. (36) and Eq. (37) respectively.

In this paper, the effective moduli of composites with interface effect are deduced by applying dilute schemes. Now we consider the composites described in Figure 2.

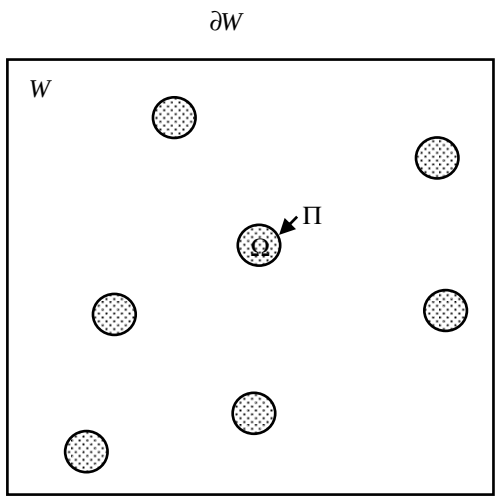

Figure 2: A schematic illustration of nanocomposites containing spherical inhomogeneities of same radius

On the boundary ∂W, the homogeneous strain and electric field boundary condition are prescribed. With the framework of dilute distribution model, the interaction between the inhomogeneities is omitted. Then, the macroscopic stress and electric displacement obtained from Eq. (36) and Eq. (37) are calculated by:

$$\tilde{\sigma} = \mathbf{c}^0 : \langle \boldsymbol{\varepsilon} \rangle - \mathbf{e}^0 \langle \mathbf{E} \rangle + v_I (\delta \mathbf{c}) : \boldsymbol{\varepsilon}^{\Omega} - v_I (\delta \mathbf{e}) \cdot \mathbf{E}^{\Omega} - (\frac{2\sigma^0}{R_0}) v_I \mathbf{I} \tag{38}$$

$$\tilde{\mathbf{D}} = \mathbf{e}^0 : \langle \boldsymbol{\varepsilon} \rangle + \mathbf{k}^0 \cdot \langle \mathbf{E} \rangle + v_I (\delta \mathbf{e}) : \boldsymbol{\varepsilon}^{\Omega} + v_I (\delta \mathbf{k}) \cdot \mathbf{E}^{\Omega} + (\frac{2k^s}{R_0}) v_I \mathbf{E}^{\Omega} \tag{39}$$

with

$$\langle \boldsymbol{\varepsilon} \rangle = \boldsymbol{\varepsilon}^0; \quad \langle \mathbf{E} \rangle = \mathbf{E}^0 \tag{40}$$

where $\mathbf{c}^0, \mathbf{e}^0, \mathbf{k}^0$ are moduli of matrix while $\mathbf{c}^1, \mathbf{e}^1, \mathbf{k}^1$ denote the moduli of the inclusion, and $\delta\mathbf{c} = \mathbf{c}^1 - \mathbf{c}^0, \delta\mathbf{e} = \mathbf{e}^1 - \mathbf{e}^0, \delta\mathbf{k} = \mathbf{k}^1 - \mathbf{k}^0$. v_I is the volume fraction of the inclusion phase.$\boldsymbol{\varepsilon}^0$ and $\mathbf{E}^0$ are uniform strain and electric field applied on ∂W.

According to the equivalent inclusion method, the inhomogeneity can be simulated by an equivalent inclusion with a uniform fictitious $\boldsymbol{\varepsilon}^*$ and $\mathbf{E}^*$. The fictitious $\boldsymbol{\varepsilon}^*$ and $\mathbf{E}^*$ can be obtained from the following equations

$$\mathbf{c}^0 : \boldsymbol{\varepsilon}^* - \mathbf{e}^0 \cdot \mathbf{E}^* + (\delta\mathbf{c}) : \boldsymbol{\varepsilon}^\Omega - (\delta\mathbf{e}) \cdot \mathbf{E}^\Omega = -(\delta\mathbf{c}) : \boldsymbol{\varepsilon}^0 + (\delta\mathbf{e}) \cdot \mathbf{E}^0 \tag{41}$$

$$\mathbf{e}^0 : \boldsymbol{\varepsilon}^* + \mathbf{k}^0 \cdot \mathbf{E}^* + (\delta\mathbf{e}) : \boldsymbol{\varepsilon}^\Omega + (\delta\mathbf{k}) \cdot \mathbf{E}^\Omega = -(\delta\mathbf{e}) : \boldsymbol{\varepsilon}^0 - (\delta\mathbf{k}) \cdot \mathbf{E}^0 \tag{42}$$

Then by substituting Eqs. (32) and (33) into Eqs. (41) and (42), we can get the expressions of $\boldsymbol{\varepsilon}^*$ and $\mathbf{E}^*$ which are related to $\boldsymbol{\varepsilon}^0$ and $\mathbf{E}^0$. Correspondingly, the uniform strain $\boldsymbol{\varepsilon}^\Omega$ and electric field $\mathbf{E}^\Omega$ inside the homogeneity can be derived immediately through Eq. (32) and Eq. (33). Bring the results of $\boldsymbol{\varepsilon}^\Omega$ and $\mathbf{E}^\Omega$ into Eq. (38) and Eq. (39), we get the expressions of $\tilde{\boldsymbol{\sigma}}$ and $\tilde{\mathbf{D}}$. According to the definitions of Eq. (34) and Eq. (35), we can obtain the expression of $\overline{\mathbf{c}^*}, \overline{\mathbf{e}^*}, \overline{\mathbf{k}^*}$, which depend on the inhomogeneity radius R_0.

5 Numerical results

5.1 Local electroelastic fields

To numerically illustrate the features of the results obtained above, we now consider a spherical inclusion undergoing uniform $\boldsymbol{\varepsilon}^*$ and $\mathbf{E}^*$ embedded in an infinite matrix which is transverse isotropic. PZT-5 material is considered, and its electroelastic constants are listed in Table 1. The interface properties can be obtained through atomistic caculations. However, due to lack of such work on piezoelectric materials, we choose $\sigma^0 = 0.5\text{J / m}^2$ and $k^s = 4.5 \times 10^{-17} c^2/N \cdot m^2$ as an approximation.

The variation of the component of electric field and strain inside the inclusion with the inclusion radius R_0 is plotted in Fig. 3 and Fig. 4, respectively. The superscript "c" denotes the value without the interface effect. One can figure out that when R_0 is in the range of several nanometers, both the electric field and strain deviate from their classical solutions, while they approach to their classical solutions with the increase of R_0. These figures show that the interface effect is significant on the strain and electric fields in nanometer scale.

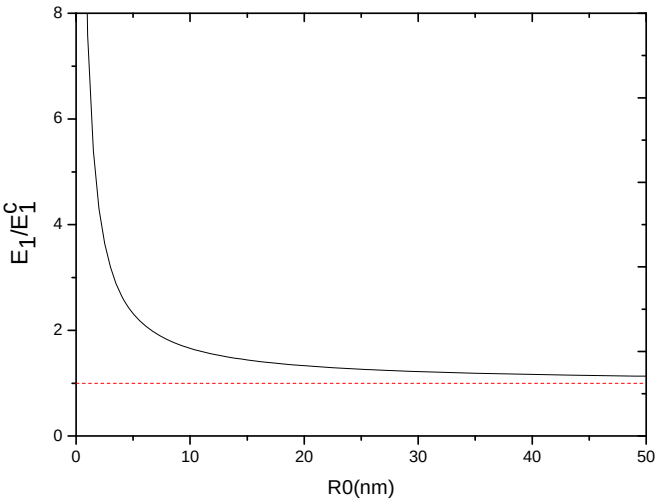

Figure 3: Electric field inside inclusion as a function of inclusion radius

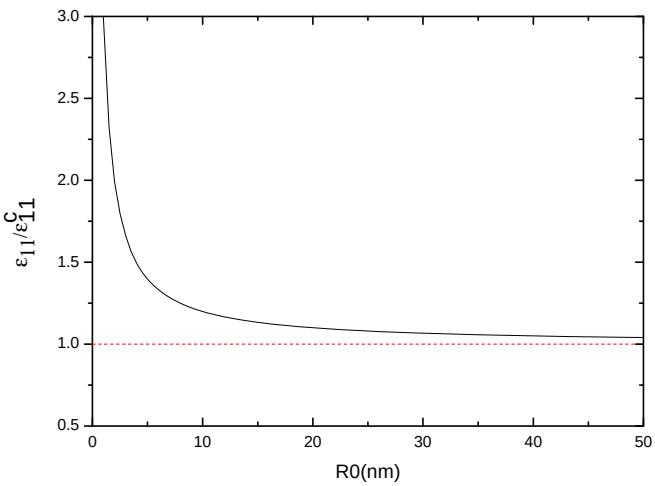

Figure 4: Strain inside inclusion as a function of inclusion radius

5.2 Effective electroelastic moduli

Here as an example, we choose PZT-5H as the inhomogeneity and PZT-5 as the matrix. The electroelastic constants of the inhomogeneity and matrix are listed in Table 1. Using the results obtained in Section 3 and 4, the following procedures are taken:

Table 1: Electroelastic material properties

	c_{11} (Gpa)	c_{12} (Gpa)	c_{13} (Gpa)	c_{33} (Gpa)	c_{44} (Gpa)	e_{31} (C / m^2)	e_{33} (C / m^2)	e_{15} (C / m^2)	κ_{11}/κ_0	κ_{33}/κ_0
PZT-5	121	75.4	75.2	111	21.1	-5.4	15.8	12.3	916	830
PZT-5H	126	55	53	117	35.3	-6.5	23.3	17.0	1706.2	1468.9

$$\kappa_0 = 8.85 \times 10^{-12} (\mathrm{C}^2 / \mathrm{Nm}^2),$$

which is the permittivity of free space.

(a) Only $\varepsilon_{33}^0 \neq 0$

From Eq.(38), one obtains

$$\begin{aligned}\tilde{\sigma}_{33} &= c_{33}^0 \varepsilon_{33}^0 + v_I[(c_{13}^1 - c_{13}^0)\varepsilon_{11}^\Omega + (c_{13}^1 - c_{13}^0)\varepsilon_{22}^\Omega + (c_{33}^1 - c_{33}^0)\varepsilon_{33}^\Omega] \\ &- v_I[(e_{33}^1 - e_{33}^0)E_3^\Omega] - (\tfrac{2\sigma^0}{R_0})v_I = \bar{c}_{33}^* \varepsilon_{33}^0\end{aligned} \tag{43}$$

(b) Only $E_3^0 \neq 0$

From Eq.(39), one obtains

$$\begin{aligned}\tilde{\sigma}_{11} &= -e_{31}^0 E_3^0 + v_I[(c_{11}^1 - c_{11}^0)\varepsilon_{11}^\Omega + (c_{12}^1 - c_{12}^0)\varepsilon_{22}^\Omega + (c_{13}^1 - c_{13}^0)\varepsilon_{33}^\Omega] \\ &- v_I(e_{31}^1 - e_{31}^0)E_3^\Omega - (\tfrac{2\sigma^0}{R_0})v_I = -\bar{e}_{31}^* E_3^0\end{aligned} \tag{44}$$

$$\begin{aligned}\tilde{D}_3 &= k_{33}^0 E_3^0 + v_I[(e_{15}^1 - e_{15}^0)\varepsilon_{12}^\Omega + (e_{33}^1 - e_{33}^0)\varepsilon_{13}^\Omega] \\ &+ v_I(k_{33}^1 - k_{33}^0)E_3^\Omega + (\tfrac{2k^s}{R_0})v_I E_3^\Omega = \bar{k}_{33}^* E_3^0\end{aligned} \tag{45}$$

According to Eq. (43), (44) and (45), we plot the value of $\bar{c}_{33}^*/c_{33}^*$, $\bar{e}_{31}^*/e_{31}^*$, $\bar{k}_{33}^*/k_{33}^*$ versus the radius of the inhomogeneity R_0 and interface parameters in Fig. 5-Fig. 8 respectively. Here, c_{33}^*, e_{31}^* and k_{33}^* are the classical effective electroelastic constants without interface effect. Fig. 5 shows that the effective elastic moduli depends on size dramatically when R_0 is on the scale of nanometer. $\bar{c}_{33}^*/c_{33}^*$ increases with increasing the inhomogeneity size and approaches to the classical solution. For the same inhomogeneity size, the value of $\bar{c}_{33}^*/c_{33}^*$ decreases when σ^0 increases.

Meanwhile, $\bar{c}^*_{33}/c^*_{33}$ appraoches to 1 (the calssical value) more quickly for a larger σ^0. The similar conclusions can be obtained for effective piezoelectric constant which are shown in Fig.6. By the way, we found that the values of k^s have negligible effects on effective elastic constants and piezoelectric constants.

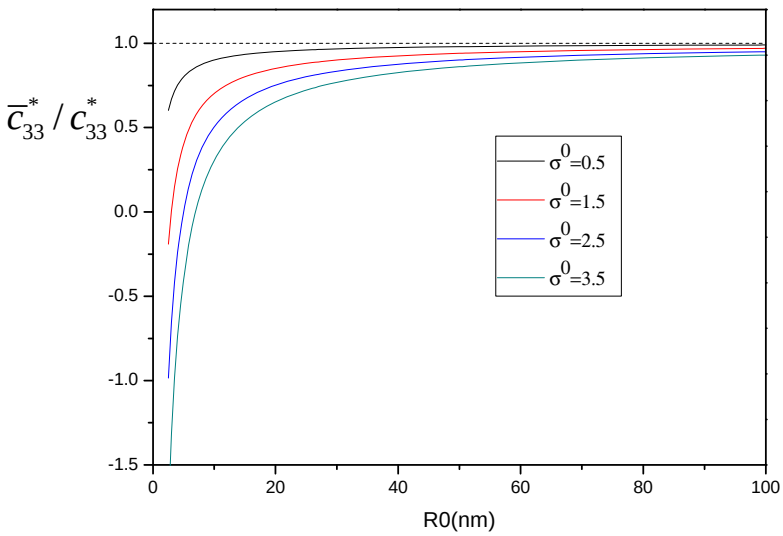

Figure 5: Effective elastic modulus as a function of interface properties and inhomogeneity radius

Fig.7 gives the effective dielectric modulus versus k^s and R_0 when $\sigma^0 = 0.5\text{J / m}^2$, while Fig.8 gives the effective dielectric modulus versus σ^0 and R_0 when $k^s = 4.5 \times 10^{-17} c^2/N \cdot m^2$. One can see from the two figures that, first, the value of $\bar{k}^*_{33}/k^*_{33}$ is size dependent and deviate considerably from the classical solution when the radius of inhomogeneities are reduced to a few nanometers. Second, for the same inhomogeneity size, the effective dielectric modulus decreases with the increase of k^s when residual interface stress is certain. Third, for the same inhomogeneity size, the effective dielectric modulus increases with the increase of σ^0 when interface dielectric modulus is constant. Fourth, the effect of interface properties becomes negligible for sufficiently large size of inhomogeneities.

6 Conclusions

The interface effect is incorporated with the piezoelectric inclusion problems to determine size-dependent local electroelastic fields and effective electroelastic moduil of nanocomposites. Based on the theory of Gurtin-Murdoch interface model and

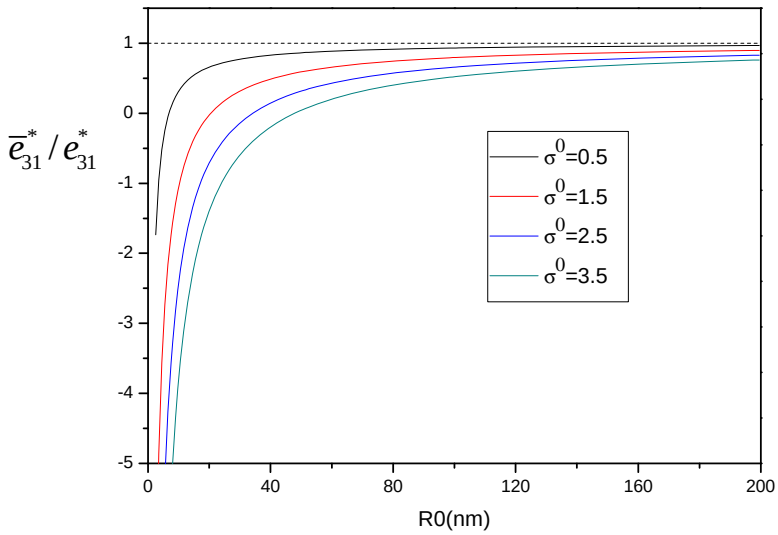

Figure 6: Effective piezoelectric modulus as a function of inhomogeneity radius

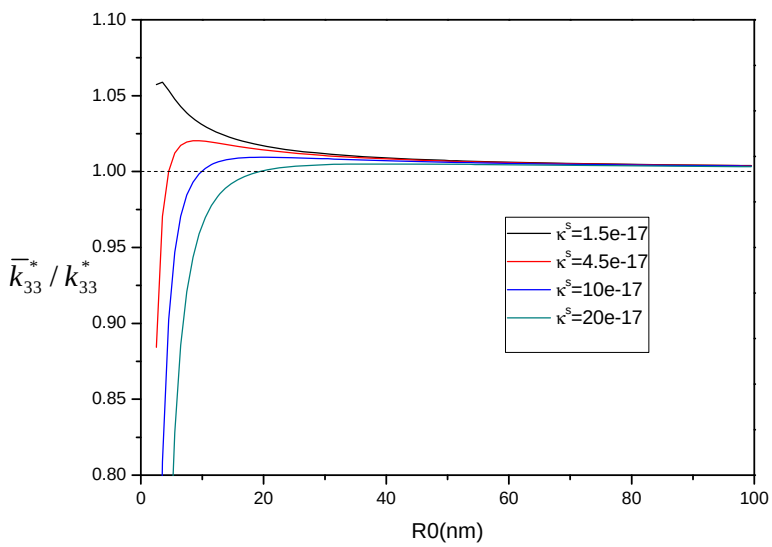

Figure 7: Effective dielectric modulus as a function of interface dielectric constant and inhomogeneity radius when $\sigma^0 = 0.5\text{J} / \text{m}^2$

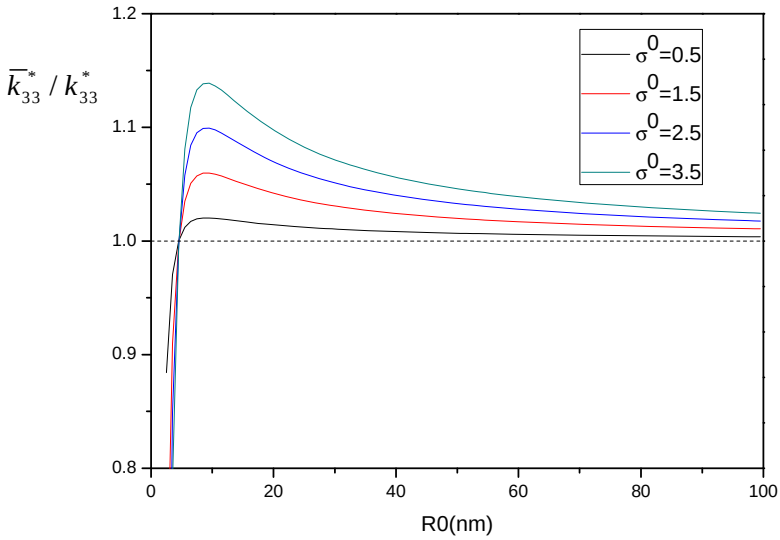

Figure 8: Effective dielectric modulus as a function of residual interface stress and inhomogeneity radius when $k^s = 4.5 \times 10^{-17} c^2/N \cdot m^2$

generalized electromechanical Young-Laplace equations, general formulas of electroelastic fields in matrix and inclusion are presented. For a spherical inclusion in transversely isotropic piezoelectric medium, we gave the closed-form solution of the electroelastic fields inside the inclusion which, unlike the classical results, are size-dependent. We also proved that the electroelastic fields including interface effect are uniform when eigenstrain and eigen electric field are uniform. Using the obtained results, effective elecroelastic moduli of piezoelectric nanocomposites are investigated by the dilute approach. The numerical results reveal that the interface effect is significant when the size of the inhomogeneity is on the scale of nanometer and the interface effect becomes negligible for large inhomogeneity in which the effective electroelastic constants approach to the classical ones.

The effective modulus are shown to be functions of the interface parameters and size of the nano-inhomogeneities. The present results are useful in understanding the interface effect on the overall response of nano-piezocomposites, and provide theoretical guidance for engineering design and application of nanostructures.

Acknowledgement: The supports from National Natural Science Foundation of China (Grants No. 11025209, 10972173, 11072184, and 11021202) are appreciated.

Appendix

The corresponding components of the piezoelectric Green's functions $\mathbf{G}^1, \mathbf{G}^2, \mathbf{G}^3, \mathbf{G}^4$ are recorded as$G_{kp}, G_{4p}, G_{k4,}G_{44}$, which are defined by (Biao, 1992):

$$C_{ijkl}G_{kp,lj} + e_{mij}G_{4p,mj} = -\delta_{ip}\delta(y-x)$$

$$e_{jkl}G_{kp,lj} - \kappa_{jk}G_{4p,jk} = 0$$

$$C_{ijkl}G_{k4,lj} + e_{kij}G_{44,kj} = 0$$

$$e_{jkl}G_{k4,lj} - \kappa_{jk}G_{44,jk} = -\delta(y-x)$$

The components of piezoelectric Eshelby tensors are as following:

$$\mathbf{S}^1 \equiv S_{mnab} = -\frac{1}{2}\left\{C_{ijab}\int_{\Omega}[G_{mj,in} + G_{nj,im}]dV + e_{iab}\int_{\Omega}[G_{m4,in} + G_{n4,im}]dV\right\}$$

$$\mathbf{S}^2 \equiv S_{mn4b} = \frac{1}{2}\left\{k_{ib}\int_{\Omega}[G_{m4,in} + G_{n4,im}]dV - e_{bij}\int_{\Omega}[G_{mj,in} + G_{nj,im}]dV\right\}$$

$$\mathbf{S}^3 \equiv S_{4nab} = -\left\{C_{ijab}\int_{\Omega}G_{4j,in}dV + e_{iab}\int_{\Omega}G_{44,in}dV\right\}$$

$$\mathbf{S}^4 \equiv S_{4n4b} = \left\{k_{ib}\int_{\Omega}G_{44,in}dV - e_{bij}\int_{\Omega}G_{4j,in}dV\right\}$$

The expressions of the four interaction tensors $\mathbf{T}^1, \mathbf{T}^2, \mathbf{T}^3, \mathbf{T}^4$ are as follows:

$$\mathbf{T}^1 \equiv T_{ijkl} = -\frac{1}{2}\int (G_{jk,li} + G_{jl,ki})dv$$

$$\mathbf{T}^2 \equiv T_{i4kl} = -\frac{1}{2}\int (G_{4k,li} + G_{4l,ki})dv$$

$$\mathbf{T}^3 \equiv T_{ij4l} = -\int G_{J4,li}dv$$

$$\mathbf{T}^4 \equiv T_{i44l} = -\int G_{44,li}dv$$

References

Chen, T. (2008): Exact size-dependent connections between effective moduli of fibrous piezoelectric nanocomposites with interface effects. *Acta Mechanica* 196, 205-217.

Chen, T., Dvorak, G. J., Yu, C. C. (2007): Size-dependent elastic properties of unidirectional nano-composites with interface stresses. *Acta Mechanica* 188, 39-54.

Chen, T. Y., Dvorak, G. J. (2006): Fibrous nanocomposites with interface stress: Hill's and Levin's connections for effective moduli. *Applied Physics Letters* 88, 211912.

Chen, T. Y., Dvorak, G. J., Yu, C. C. (2007): Solids containing spherical nano-inclusions with interface stresses: Effective properties and thermal-mechanical connections. *International Journal of Solids and Structures* 44, 941-955.

Cherkaoui, M., Capolungo, L. (2009): Innovative Combinations of Atomistic and Continuum: Plastic Deformation of Nanocrystalline Materials. *Atomistic and Continuum Modeling of Nanocrystalline Materials* 112, 353-378.

Duan, H., Wang, J., Huang, Z., Karihaloo, B. (2005a): Size-dependent effective elastic constants of solids containing nano-inhomogeneities with interface stress. *Journal of the Mechanics and Physics of Solids* 53, 1574-1596.

Duan, H., Wang, J., Huang, Z., Karihaloo, B. L. (2005b): Eshelby formalism for nano-inhomogeneities. *Proceedings of the Royal Society A: Mathematical, Physical and Engineering Science* 461, 3335-3353.

Duan, H. L., Wang, J., Karihaloo, B. L. (2008): Theory of Elasticity at the Nanoscale. *Advances in Applied Mechanics* 42, 1-68.

Dunn, M. L., Taya, M. (1993): An analysis of piezoelectric composite materials containing ellipsoidal inhomogeneities. *Proceedings of the Royal Society of London. Series A: Mathematical and Physical Sciences* 443, 265-287.

Dunn, M. L., Wienecke, H. (1997): Inclusions and inhomogeneities in transversely isotropic piezoelectric solids. *International Journal of Solids and Structures* 34, 3571-3582.

Gurtin, M., Weissmüller, J., Larche, F. (1998): A general theory of curved deformable interfaces in solids at equilibrium. *Philosophical Magazine A* 78, 1093-1109.

Hu, S., Shen, S. (2009): Electric Field Gradient Theory with Surface Effect for Nano-Dielectrics. *CMC: Computers, Materials, & Continua* 13, 63-88.

Hu, S., Shen, S. (2010): Variational principles and governing equations in nano-dielectrics with the flexoelectric effect. *Science China-Physics Mechanics & Astronomy* 53, 1497-1504.

Huang, G., Yu, S. (2006): Effect of surface piezoelectricity on the electromechanical behaviour of a piezoelectric ring. *physica status solidi (b)* 243, R22-R24.

Huang, Z., Sun, L. (2007): Size-dependent effective properties of a heterogeneous material with interface energy effect: from finite deformation theory to infinitesimal strain analysis. *Acta Mechanica* 190, 151-163.

Huang, Z., Wang, J. (2007): Micromechanics of Nanocomposites with Interface Energy Effect. IUTAM Symposium on Mechanical Behavior and Micro-Mechanics of Nanostructured Materials. Springer. Printed in the Netherlands.144, 51-59.

Le-Quang, H., Bonnet, G., He, Q. C. (2010): Size-dependent Eshelby tensor fields and effective conductivity of composites made of anisotropic phases with highly conducting imperfect interfaces. *Physical Review B* 81, 064203.

Lim, C. W., Li, Z. R., He, L. H. (2006): Size dependent, non-uniform elastic field inside a nano-scale spherical inclusion due to interface stress. *International Journal of Solids and Structures* 43, 5055-5065.

Sharma, P., Ganti, S. (2004): Size-dependent Eshelby's tensor for embedded nano-inclusions incorporating surface/interface energies. *Journal of Applied Mechanics* 71, 663-671.

Sharma, P., Ganti, S., Bhate, N. (2003): Effect of surfaces on the size-dependent elastic state of nano-inhomogeneities. *Applied Physics Letters* 82, 535-537.

Shen, S. , Hu, S. (2010): A theory of flexoelectricity with surface effect for elastic dielectrics. *Journal of the Mechanics and Physics of Solids* 58, 665-677.

Tian, L., Rajapakse, R. K. N. D. (2007): Elastic field of an isotropic matrix with a nanoscale elliptical inhomogeneity. *International Journal of Solids and Structures* 44, 7988-8005.

Xiao, J., Xu, Y., Zhang, F. (2011): Size-dependent effective electroelastic moduli of piezoelectric nanocomposites with interface effect. *Acta Mechanica* 222,59-67.

Xu, Y., Shen, S. (2012): Surface Electric Gibbs Free Energy and Its Effect on the Electromechanical Behavior of Nano-Dielectrics. *CMC: Computers, Materials, & Continua* 28, 81-95.

Wang, B. (1992): Three-dimensional analysis of an ellipsoidal inclusion in a piezoelectric material. *International Journal of Solids and Structures* 29, 293-308.

Yang, F. (2006): Effect of interfacial stresses on the elastic behavior of nanocomposite materials. *Journal of Applied Physics* 99, 054306.